Ouyang Kai, Han Xiaoxiang*, Xiong Chunhua, Tang Xiujuan and Chen Qing

Water-soluble heteropolyacid-based ionic liquids as effective catalysts for oxidation of benzyl alcohol in water with hydrogen peroxide

DOI 10.1515/gps-2016-0237
Received December 29, 2016; accepted March 6, 2017; previously published online May 24, 2017

Abstract: A series of organic-inorganic composite catalysts were prepared by modifying tungstophosphoric acid ($H_3PW_{12}O_{40}$) and propyl sulfonic acid-functionalized ionic complex. The obtained water-soluble catalysts were well characterized by Fourier transform infrared spectroscopy, X-ray diffraction, thermogravimetric analysis, and nuclear magnetic resonance, and investigated for their performance as homogeneous catalysts for selective oxidation of benzyl alcohol (BzOH) with hydrogen peroxide (H_2O_2) in water. Among them, the [DMBPSH]$H_2PW_{12}O_{40}$ catalyst exhibited the best oxidative activity with a desirable benzaldehyde (BzH) selectivity of 97.0% and an excellent BzOH conversion of 98.5%. Further kinetic studies and model analysis by response surface methodology revealed that alcohols' oxidation reaction followed an apparent order of 2.2 with an activation energy of 36.18 kJ/mol. And the optimal reaction conditions were established as follows: BzOH/H_2O_2 molar ratio of 1:1.7, amount of catalyst 5.4 wt%, reaction time 3.9 h, amount of water 24 ml, and a maximum yield of BzH of 95.8%. Under optimum conditions, [DMBPSH]$H_2PW_{12}O_{40}$ catalyst showed a superior catalytic efficiency and reusability due to strong acidity and excellent surface activity.

Keywords: ionic liquid; optimization; oxidation; reaction engineering; tungstophosphoric acid.

1 Introduction

The selective oxidation of alcohols to their corresponding carbonyl compounds is one of the most important processes in fine chemical industry. Traditional methods for the oxidation of alcohols are carried out with stoichiometric amounts of organic or inorganic oxidants [1, 2]. However, these methods easily cause environmental and economic problems due to disposal of large amounts of byproducts [3]. Moreover, reactions are often performed in environmentally undesirable solvents, typically chlorinated hydrocarbons. From economic and environmental viewpoints, the development of clean and green approaches utilizing molecular oxygen or H_2O_2 as oxidant combination with recyclable catalysts for alcohol oxidation has attracted increasing attention [4, 5]. These processes are atom efficient and water is the only byproduct. Although advantages of using H_2O_2 as an oxidant during alcohol oxidation are evident, reports on this particular subject are still scarce [6].

As well known, heteropolyacids (HPAs) are a class of well-defined transition metal oxygen clusters with structural diversity. Because of their rich redox chemistry, HPAs, especially those of the Keggin series, have been revealed to be very effective in the oxidation of alcohols with H_2O_2 [7, 8]. However, HPA catalysts usually need the use of organic solvents, and cannot be recovered conveniently due to their good solubility in polar solvents. To circumvent this problem, an alternative approach is to exchange counter cation (i.e. H^+) of HPAs with various metal ions, e.g. Co^{2+}[9], Ag^+[10], or Cs^+[11] to form insoluble salts. Such solid acid catalysts show superior stability, nonetheless, the nanocrystalline size of the tertiary structure of HPA remains as a critical limitation for separation and reuse [12]. Consequently, considerable recent research interests have been focusing on the development of novel HPA-based ionic liquids (HPAILs), which showed excellent catalytic performances for their "self-seperation" and pseudo-liquid properties in esterification [13–15]. Good catalytic properties of HPAILs were also found on the selective oxidation of alcohol with aqueous H_2O_2 [16, 17]. However, these reports suffer from applying organic solvents, mass transfer limitation, low efficiency of H_2O_2 utilization, lack of generality, etc. Few efficient and catalytic oxidation processes with H_2O_2 and water as solvents that proceed under mild conditions are known [18–20].

***Corresponding author: Han Xiaoxiang,** Department of Applied Chemistry, Zhejiang Gongshang University, Hangzhou 310018, China, e-mail: hxx74@126.com
Ouyang Kai, Xiong Chunhua and Chen Qing: Department of Applied Chemistry, Zhejiang Gongshang University, Hangzhou 310018, China
Tang Xiujuan: College of Environmental Science and Engineering, Zhejiang Gongshang University, Hangzhou 310018, China

Herein, we describe the synthesis of a series of organic-inorganic composite catalysts by ionic liquid and HPA as precursors. More specifically, the HPAILs catalysts were prepared by combining SO_3H-functionalized ionic liquid with high molecular volume [N,N-dimethyl(benzyl)-ammonium propyl sulfobetaine (DMBPS)] and Keggin-type structure of tungstophosphoric acid ($H_3PW_{12}O_{40}$; TPA) under different composition ratios. The resultant nontoxic, low-cost, and water-soluble HPAILs catalysts were characterized by a variety of analytical and spectroscopic techniques and exploited for oxidation of benzyl alcohol with 30% H_2O_2 in water. In particular, this catalytic reaction was carried on biphasic system. After the reaction, the catalyst was easily recycled from the aqueous and the products were separated from the organic phase at the same time. So that the reaction is safe, efficient and environmentally friendly. Also, it was demonstrated that the catalyst was efficient and sustainable.

2 Materials and methods

2.1 Catalyst preparation

All chemicals were analytical grade and were used without further purification unless otherwise stated. The organic-inorganic composite catalysts were prepared following the procedures reported elsewhere [15, 21]. In brief, equal amounts of $H_3PW_{12}O_{40}$ (KuishanXingbang Technology Co., Ltd., Jiangsu, China) and desirable ionic liquid DMBPS, were first dissolved in water, then, the mixed solution was stirred at 363 K for 24 h. After removing the water, the obtained solid product was washed with diethyl ether followed by drying under a vacuum (Shanghai Boxun Industrial Co., Ltd., China). The products are denoted as $[DMBPSH]_xH_{3-x}PW_{12}O_{40}$ in which x means the molar ratio of DMBPS/TPA changing from 1.0 to 3.

2.2 Catalyst characterization

The FT-IR spectra were measured on Bruker IFS28 spectrometer using anhydrous KBr technique pellet as standard. The crystal phases of the synthesized catalysts were employed by a Bruker D8 ADVANCE X-ray diffractometer (XRD, Bruker Co., Germany) equipped with a graphite monochromator using Cu Kα radiation (40 kV, 20 mA) over the 2θ range of 5–80°. The themogravimetric (TG) analyses were carried out with TG209 (NETISCH) in flowing N_2 by heating the sample from room temperature to 873 K at a rate of 10 K/min. ^1H and ^{13}C NMR spectra were employed on a Bruker AV-500 spectrometer. Solid-state ^{31}P MAS NMR measurements were performed on a Bruker-Biospin Avance-III 500 spectrometer at a Larmor frequency of 202.46 MHz using a 4 mm double-resonance MAS probehead. ^{31}P spectra were acquired by a single-pulse sequence under a sample at spinning rate of 12 kHz with an excitation pulse of 1.5 μs (π/6 pulse) and a recycle delay of 10 s. The ^{31}P chemical shifts were referenced to that of 85% H_3PO_4 aqueous solution. The detail of sample processing was prepared following the procedure outlined in literature [22].

2.3 Catalytic testing

The selectivity oxidation reactions were carried out in a 100 ml three-necked flask equipped with reflux condenser. The procedure was as follows: benzyl alcohol (BzOH, Sinopharm Chemical Reagent Co., Ltd., Shanghai, China) (5.40 g, 0.05 mol), 30% H_2O_2 (H_2O_2, XLong Scientific Co., Ltd., Shanghai, China) (11.58 g, 0.1 mol), catalyst (0.27 g, 5 wt%), and water (20 ml) were added in the flask. The reaction mixture was heated to 393 K for 3 h in the oil bath. The mixture was then cooled to the room temperature and the catalyst was separated from the mixture. The spent catalyst was washed by diethyl ether for reuse. The products were extracted by ethyl acetate and then filtered with a 0.22 μ-organic membrane before being analyzed by gas chromatography. Chemical analysis of the products was performed by gas chromatography (Agilent6890NGC), equipped with a FID detector and HP-5 capillary column. Reactants and products were identified by comparison with authentic samples. Diphenyl was used as the internal standard. Catalytic performances of various organic-inorganic composite catalysts during oxidation of benzyl alcohol (BzOH) with H_2O_2 were listed in Table 1.

2.4 Experimental design and mathematical model

An experimental design for a series of experimental variables based on RSM (Design-Expert® Version 8.0.7.1) was used for the production of benzaldehyde (BzH) by oxidation of BzOH over the organic-inorganic composite ($[DMBPSH]_xH_{3-x}PW_{12}O_{40}$) catalysts. A Box-Behnken design (BBD) was utilized to study the effect of four independent process variables, namely BzOH/H_2O_2 molar ratio (x_1), amount of catalyst (x_2), reaction time (x_3), and amount of water (x_4). All factors in the experiment were established and coded into three levels –1, 0, and +1, as defined in Table 2. A 3^4 full-factorial central composite design with three coded levels was utilized, for which 29 experimental sets (5 central points and 24 factorial) were adopted, as depicted in Table 3. The coded values of these factors were obtained according to Eq. (1) [23, 24]:

$$x_i = \frac{X_i - X_0}{\Delta X_i} \quad (1)$$

Table 1: Catalytic performances of various catalysts during oxidation of BzOH with H_2O_2 [reaction conditions: BzOH/H_2O_2 molar ratio = 1:2 (mol/mol); amount of catalyst = 5 wt%; reaction time = 3 h; amount of water = 20 ml; temperature 393 K].

Catalyst	Conversion (%)[a]	Selectivity (%)[a]	Yield (%)
$H_3PW_{12}O_{40}$	62.3	93.5	60.4
DMBPS	5.4	99.7	5.3
$[TEAPSH]H_2PW_{12}O_{40}$[b]	68.1	95.6	65.1
$[DMPPSH]H_2PW_{12}O_{40}$[c]	89.5	95.3	85.3
$[DMBPSH]H_2PW_{12}O_{40}$	94.4	96.4	91.6
$[DMBPSH]_2HPW_{12}O_{40}$	92.5	95.6	88.4
$[DMBPSH]_3PW_{12}O_{40}$	90.6	95.7	86.7

[a]Analyzed by GC.
[b]TEAPS, Triethylammonium propyl sulfobetaine.
[c]DMPPS, N,N-dimethyl(phenyl)ammonium propyl sulfobetaine.

Table 2: List of symbols for various experimental variables and corresponding coded levels and ranges adopted in the experimental designs.

Factors	Symbol	Range and level		
		−1	0	1
BzOH/H_2O_2 molar ratio (mol/mol)	x_1	1:1	1:2	1:3
Amount of catalyst (wt%)	x_2	4	5	6
Reaction time (h)	x_3	3	4	5
Amount of water (ml)	x_4	15	20	25

Table 3: List of experimental design and response values obtained for oxidation of BzOH over [DMBPSH]$H_2PW_{12}O_{40}$ catalyst.

Experiment no.	Variable and level				Yield (%)	
	x_1	x_2	x_3	x_4	Experimental	Calculated
1	−1	−1	0	0	88.40	88.63
2	1	−1	0	0	82.42	81.78
3	−1	1	0	0	90.89	90.80
4	1	1	0	0	83.76	82.80
5	0	0	−1	−1	86.68	85.59
6	0	0	1	−1	91.23	90.44
7	0	0	−1	1	90.34	90.41
8	0	0	1	1	89.92	90.29
9	−1	0	0	−1	86.50	87.10
10	1	0	0	−1	79.31	80.97
11	−1	0	0	1	92.25	90.74
12	1	0	0	1	82.47	82.02
13	0	−1	−1	0	86.74	86.87
14	0	1	−1	0	90.86	90.72
15	0	−1	1	0	91.20	91.49
16	0	1	1	0	90.81	90.83
17	−1	0	−1	0	88.90	89.52
18	1	0	−1	0	77.59	78.02
19	−1	0	1	0	87.66	87.81
20	1	0	1	0	84.50	84.46
21	0	−1	0	−1	90.73	90.25
22	0	1	0	−1	87.79	87.89
23	0	−1	0	1	88.16	88.63
24	0	1	0	1	93.12	94.18
25	0	0	0	0	94.53	95.07
26	0	0	0	0	94.87	95.07
27	0	0	0	0	95.63	95.07
28	0	0	0	0	94.80	95.07
29	0	0	0	0	95.52	95.07

where x_i is the independent variable coded value, X_i, X_0, and ΔX_i (i=1–4) represent the real, central, step-change value of the associated variable, respectively.

The second-order model equation given by RSM was used to reveal the interactive effects between experimental variables to optimize the reaction process, and to predict the yield of BzH, which represents the responses of the experimental design. The quadratic equation model was described according to Eq. (2):

$$Y = \beta_0 + \sum_{i=1}^{4} \beta_i x_i + \sum_{i=1}^{4} \beta_{ii} x_i^2 + \sum_{i<j}^{4} \beta_{ij} x_i x_j \quad (2)$$

where Y is the process predicted response, x_i and x_j (i and j=1–4) denote the uncoded independent variables, while β_0, β_i, β_{ii}, and β_{ij} represent the regression coefficients for the corresponding variables. The validity and significance of the proposed model were assessed through statistical parameters based on analysis of variance (ANOVA) method.

2.5 Kinetic studies

The reaction rate (r) for selectivity oxidation of BzOH to BzH can be expressed as follows:

$$r = -\frac{dC_A}{dt} = k' C_A^{\alpha} C_B^{\beta} \quad (3)$$

where C_A, C_B, represent the instant concentrations of BzOH, H_2O_2, respectively; k' is the forward rate constant; α, β are the reaction orders of BzOH, H_2O_2, respectively. Taking the natural logarithm, Eq. (3) may further be expressed as:

$$\ln r = \ln k + \alpha \ln C_A \quad (4)$$

where $k = k' C_B^{\beta}$ refers to the modified rate constant. After a series of calculation, the values of k and α for the oxidation reaction at different temperatures could be obtained. Also, the Arrhenius equation which relates reaction rate constant with activation energy was defined as:

$$\ln k = \ln k_0 - \frac{E_a}{R} \frac{1}{T} \quad (5)$$

where k_0 presents the pre-exponential factor, R is the gas constant, and T represents the reaction temperature.

3 Results and discussion

3.1 Characterization of catalysts

The FTIR spectra of pristine $H_3PW_{12}O_{40}$ and $[DMBPSH]_xH_{3-x}PW_{12}O_{40}$ (x=1, 2, 3) catalysts were recorded, respectively. As exhibited in Figure S1, characteristic adsorption peaks of pristine TPA are at around 1080, 981, 889, and 804 cm^{-1} for Keggin structure, and may be attributed to the asymmetric stretching vibrations of P–O, terminal W=O, corner-sharing W–O_b–W, and edge-sharing W–O_c–W bonds, respectively [22, 25]. For all organic TPA salts, four peaks appeared distinctively, despite the fact peak intensities decreased and peak positions shifted slightly. It is demonstrated that organic TPA salts still retained the Keggin structure even after partial substitution of TPA by DMBPS. Additional bands are at 1470, 1253,

and 1203 cm^{-1}, which may be assigned to C–H bending vibrations of $-CH_2$ and $-CH_3$ groups, and asymmetric and symmetric vibrations of S=O, respectively (Figures S1C–F) [13, 26]. Extra absorption peaks at 2939 cm^{-1} may be attributed to the stretching vibrations of $-CH_2$ species. The above results verify a successful linkage between inorganic polyanions ($PW_{12}O_{40}^{3-}$; PW) and sulfonate functionalized organic cations.

The structural integrity of various organic TPA salts was further examined by XRD, as shown in Figure S2. Unlike the profile of DMBPS (Figure S2A), which showed diffraction peaks mostly in the 2θ range of 5–35°, the pristine TPA revealed the featured diffraction peaks at 10.3, 25.3, and 34.6° for Keggin-type structure with long-range order [27]. Upon incorporating DMBPS into TPA, XRD patterns of organic TPA salts similar to that of the neat TPA were observed (Figure S2C–E), except for a marginal shift of diffraction peaks toward higher 2θ values and slight decrease in peak intensity. However, no feature diffraction peaks for the pure DMBPS (Figure S2A) could be identified, suggesting the presence of a new organic salt phase with good crystallinity. Further increasing concentration of DMBPS led to notable decreases in crystallinity, which were accompanied by emerging of additional peaks in 2θ region of ca. 5.0–10.0°. The above results again verify successful incorporation of DMBPS into TPA while retaining Keggin structure with good crystallinity [10].

To investigate thermal stabilities of organic TPA salts, thermogravimetric analysis (TGA) was carried out from room temperature to 873 K at a rate of 10 K/min under nitrogen atmosphere. As all organic TPA salts showed a similar TG-DTG profile, herein, only a curve observed for $[DMBPSH]H_2PW_{12}O_{40}$ catalyst was illustrated and discussed. As shown in Figure S3C, $[DMBPSH]H_2PW_{12}O_{40}$ catalyst exhibited four distinct weight-loss peaks at 321, 432, 548 and 673–780 K, which may be ascribed to desorption of physisorbed water, loss of crystalline water, decomposition of organic moieties and collapse of Keggin structure, respectively [13, 15]. Again, these results further verify successful anchoring of DMBPS on TPA and such organic TPA salts remain stable under reaction condition. Moreover, ^1H and ^{13}C NMR spectra obtained from the $[DMBPSH]H_2PW_{12}O_{40}$ catalyst further confirmed anticipated chemical compositions with corresponding NMR data. The ^1H and ^{13}C NMR spectra of DMBPS were listed in literature [15]. $[DMBPSH]H_2PW_{12}O_{40}$: 1H NMR (500 MHz, D2O); 2.218 (m, 2H), 2.891 (t, 2H), 2.982 (s, 6H) 3.366 (t, 2H), 4.450 (s, 2H), 7.487–7.493 (m, 5H) ppm; 13C NMR (125 MHz, D2O); δ 18.43, 47.45, 49.69, 62.52, 68.61, 126.95, 129.37, 131.00, 133.01 ppm.

In addition, acidic properties of pure DMBPS and various $[DMBPSH]_xH_{3-x}PW_{12}O_{40}$ ($x=0$–3) catalysts were characterized by the solid-state ^{31}P-TMPO NMR approach [28, 29]. As shown in Figure 1, the pristine TPA exhibited ^{31}P NMR signals at resonance of adsorbed TMPO at $\delta^{31}P = 92.1$, 88.6, 82.8, –10.9, and –15.2 ppm. The resonances with $\delta^{31}P = -10.9$ and –15.2 ppm may be attributed to the $PW_{12}O_{40}^{3-}$ Keggin polyanions alone, which may also be observed for the bare TPA in the absence of TMPO. The three resonances ($\delta^{31}P = 92.1$, 88.6, and 82.8 ppm) may be attributed to TMPO adsorbed on the three Brønsted superacidic proton (H^+) sites (i.e. due to signal from $TMPOH^+$ complexes), which exceeded the chemical shift threshold for superacidity (86 ppm) [26, 27]. DMBPS showed practically no acidity in the presence of adsorbed TMPO (Figure 1G). The ^{31}P signals at 42 ppm observed for the DMBPS was mainly due to bulk TMPO [27, 28].

Upon incorporating DMBPS into TPA, the acidic strength (i.e. $\delta^{31}P$ value) decreased from beyond 86 ppm to the high-field (Figure 1B–D). Eventually, as all available proton sites were intercalated with DMBPS ($x=3$; Figure 1D), broad ^{31}P signals at 82 ppm with lower peak area was observed, indicating an overall decrease in both acidic strength and concentration of acid sites compared to the pristine TPA. Moreover, the peak at ca. 66 ppm

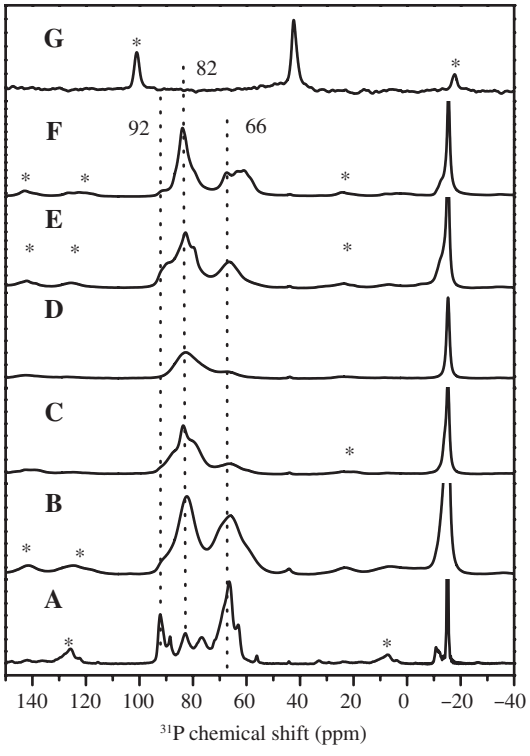

Figure 1: ^{31}P NMR spectra of TMPO adsorbed on (A) the pristine $H_3PW_{12}O_{40}$ and various organic TPA catalysts: (B) $[DMBPSH]H_2PW_{12}O_{40}$, (C) $[DMBPSH]_2HPW_{12}O_{40}$, (D) $[DMBPSH]_3PW_{12}O_{40}$, and (E) pure DMBPS. The asterisks in the spectra denote spinning sidebands.

for the organic composite salts may be ascribed to the presence of $(TMPO)_nH^+(n>1)$ adducts, in which an acid site was associated with more than one probe molecule [27]. The above results implied that incorporated DMBPS tended to provoke an effective averaging of Brønsted acidic strength, leading to lowering overall acidity. It was anticipated that the presence of DMBPS not only facilitated elimination of available protic sites but also promoted segregation of TPA Keggin units, which was favorable for molecular transport [13]. From the area of peak, we also found the order of Brønsted acidity for organic TPA salts was $[DMBPSH]H_2PW_{12}O_{40} \approx [DMPPSH]H_2PW_{12}O_{40} > [TEAPSH]H_2PW_{12}O_{40}$.

3.2 Selectivity oxidation of benzyl alcohol with hydrogen peroxide

The acidity order of sample was consistent with their activity order in some acid-catalyzed reactions. Oxidation with H_2O_2 is a typical acid-catalyzed reaction for enhancing the oxidation capacity of H_2O_2 under strong acidic conditions [30]. Table 1 listed the results of oxidation of BzOH with H_2O_2 over the synthesized organic TPA salts. As shown in Table 1, DMBPS showed negligible conversion and BzH yield. The organic TPA salts showed satisfactory catalytic performances compared to the pristine TPA even though the pristine TPA was found to possess the strongest Brønsted acidity. Among various organic TPA salts, the $[DMBPSH]H_2PW_{12}O_{40}$ catalyst exhibited the best catalytic activity (conversion 94.4%, selectivity 96.4%, and yield 91.6%). Compared with its DMBPS-functionalized TPA counterparts, $[DMBPSH]H_2PW_{12}O_{40}$ with the most available (two) Brønsted acidic protons (hence strongest acidity) showed superior activity compared to $[DMBPSH]_2HPW_{12}O_{40}$ (one residual H^+) and $[DMBPSH]_3PW_{12}O_{40}$. According to the results obtained, we thought the strong acidity of $[DMBPSH]_xH_{3-x}PW_{12}O_{40}$ was responsible for high catalytic activity. However, higher ultra-strong Brønsted acidity was not readily favorable for catalytic oxidation of alcohol. Comparing $[MH]H_2PW_{12}O_{40}$ with M = DMBPS to its counterparts with M = DMPPS and TEAPS, their catalytic activity follows the trend: $[DMBPSH]H_2PW_{12}O_{40} > [DMPPSH]H_2PW_{12}O_{40} > [TEAPSH]H_2PW_{12}O_{40}$. Although [DMPPSH]-$H_2PW_{12}O_{40}$ catalyst possesses similar acidity to $[DMBPSH]H_2PW_{12}O_{40}$ catalyst (see Figure 1), it exhibited less catalytic performance during the oxidation reaction. The SO_3H-functionalized ionic liquid catalyst with high molecular volume showed excellent surface activity and solubility in water, which made a problem of hydrophobic alcohol being immiscible in aqueous H_2O_2 [31]. The oxidation can be carried out with good catalytic activity for homogenous condition without adding any phase transfer catalyst. The different catalytic activity of $[DMBPSH]H_2PW_{12}O_{40}$ and $[DMPPSH]H_2PW_{12}O_{40}$ catalysts may be related to catalyst structure. DMBPS showed higher molecular volume than DMPPS, which made $[DMBPSH]H_2PW_{12}O_{40}$ catalyst with good catalytic activity for higher surface activity. $[TEAPSH]H_2PW_{12}O_{40}$ catalyst exhibited the worst catalytic performance for low acidity and low surface activity.

3.3 Process optimization

As $[DMBPSH]H_2PW_{12}O_{40}$ catalyst was found to exhibit the best catalytic performance among various TPA IL examined, it was chosen for further process optimization study. The effects of independent experimental variables, such as catalyst amount, benzyl alcohol/hydrogen peroxide ($BzOH/H_2O_2$) molar ratio, reaction time, and water amount were investigated. Among them, the amount of catalyst played a key role during oxidation. Figure 2A showed the effect of $[DMBPSH]H_2PW_{12}O_{40}$ amount on catalytic activity during the oxidation of BzOH with H_2O_2. The BzOH conversion gradually increased from ca. 66.2% to 94.0% as the amount of catalyst in the reaction mixture increased from 3 to 7 wt%. This may be attributed to a progressive increase in active acid sites available for catalyzing the oxidation reaction. Meanwhile, the yield of BzH increased initially with increasing catalyst amount, and it reached a maximum (91.6%) at a catalyst amount of 5 wt%. Further increasing the amount of catalyst resulted in a notable decrease in BzH yield. This is attributed to an excessive amount of acid sites present in the reaction system, which provoked formation of byproducts due to undesirable oxidation of BzH and other reactions.

Figure 2B showed variations of $BzOH/H_2O_2$ molar ratio on BzOH conversion and BzH yield over the $[DMBPSH]H_2PW_{12}O_{40}$ catalyst. The BzH yield increased with increasing amount of reactant, reaching a maximum of 91.6%, at around $BzOH/H_2O_2 = 1{:}2$. This indicated that a desirable amount of H_2O_2 oxidant was favorable for driving the equilibrium towards formation of BzH. Nevertheless, further increasing the amount of H_2O_2 led to dilution of the reactant (BzOH) and catalyst, resulting in undesirable oxidation of BzH, and hence, lowering BzH yield.

The effect of reaction time on BzOH conversion and BzH yield was examined under the reaction conditions of $BzOH/H_2O_2 = 1{:}2$, catalyst amount = 5 wt%, water amount = 20 ml, and reaction temperature = 393 K while

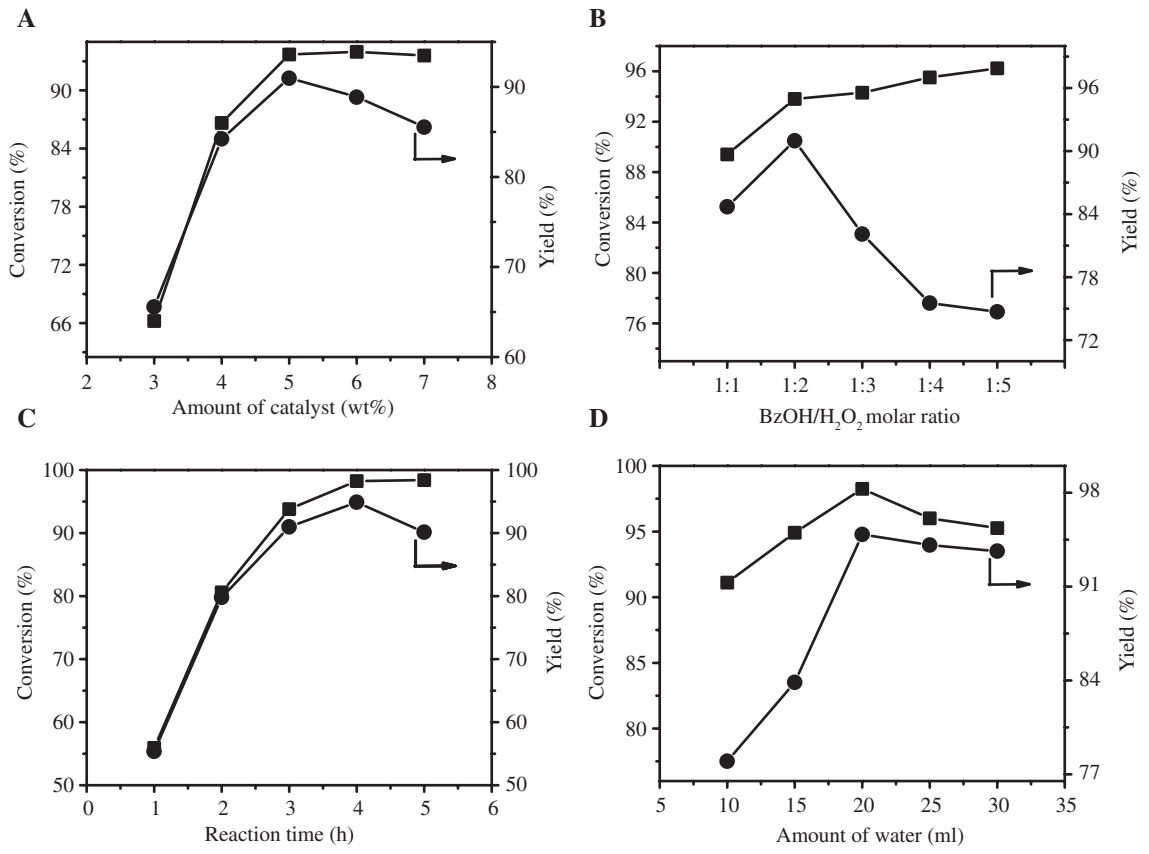

Figure 2: Effects of (A) amount of catalysts, (B) benzyl alcohol to hydrogen peroxide molar ratio, (C) reaction time, and (D) amount of water on conversion (●) and benzaldehyde yield (■), during oxidation of BzOH with H_2O_2 over the $[DMBPSH]H_2PW_{12}O_{40}$ catalyst.

varying the reaction time from 1 to 5 h. As shown in Figure 2C, both BzOH conversion and BzH yield increased with reaction time and a good yield (94.8%) was reached at 4 h. Further increasing the reaction time, BzOH conversion rate remained unchanged, indicating that the reaction reached a balance at 4 h. However, a progressive decrease in the yield of BzH was due to depletion of BzOH and excessive BzH occupied the catalytic activity sites, so that the oxidation of BzH was observed at prolonged reaction time, thus, affecting product yield.

Based on experimental results described earlier, the effect of water amount on catalytic activity during the oxidation reaction was also investigated. As shown in Figure 2D, BzOH conversion and BzH yield were found to increase consistently with increasing amount of water in the reaction system, leading to an optimal BzH selectivity (96.6%) and a conversion of 98.2% at an amount of 20 ml. The presence of suitable amount of water as solvents is favorable for adsorption and/or activation of oxidant [32–34]. After reaction, most products can be separated by simple decantation, and water-soluble catalyst solution could be recycled. Nevertheless, as water amount exceeding 20 ml, the reaction activity decreased due to dilution of catalyst system. The deficiency in acid sites led to decrease of catalytic activity.

3.4 RSM experiments and studies

A factorial design of experiments and response surface methodology (RSM) were adopted to evaluate interactive effects of the experimental variables and to optimize reaction process. Furthermore, ANOVA methods were used to evaluate the effect of process variables in the esterification reaction. To verify models, 29 runs of experiment were needed and the obtained response values were shown in Table 3. Obviously there was no observable difference between experimental values and calculated values in Table 3. Regression analysis is generally used to fit an empirical model with collected response variable data. By multiple regression analysis, response displayed in Table 3 was related with four independent factors (BzOH/H_2O_2 molar ratio, amount of catalyst, reaction time, and amount of water). And yield (Y) may be correlated with

independent experimental variables by a quadratic model, which can be expressed as:

$$Y = +95.07 - 3.71x_1 + 0.80x_2 + 1.18x_3 + 1.17x_4 - 7.05x_1^2 - 2.02x_2^2 - 3.07x_3^2 - 2.82x_4^2 - 0.29x_1x_2 + 2.04x_1x_3 - 0.65x_1x_4 - 1.13x_2x_3 + 1.98x_2x_4 - 1.24x_3x_4 \quad (6)$$

where x_1, x_2, x_3, and x_4 were coded values, representing four experimental variables, namely $BzOH/H_2O_2$ molar ratio, amount of catalyst, reaction time, and amount of water respectively. The coefficient of determination (R^2) obtained from regression of Eq. (6) was 0.9802, indicating that the model was reliable and there was no obvious difference between the predicted and experimental values.

Using standard ANOVA, the model was tested to estimate whether the quadratic model and model terms were significant or not. The statistical analysis, shown in Table 4, presented that the Model *F*-value for selectivity oxidation yield (49.58) was much higher than the tabular *F*-value at 5% level of significance. Also, the "Pred R-Squared" of 0.8924 completely agrees with the "Adj R-Squared" of 0.9605, meaning that the model is significant and predictive value fits the model. Besides, coefficient of variation was 1.05%, relatively low value also demonstrated that the model owned a better precision and experiment process was reliable. As shown in Table 4, ANOVA results confirm a satisfactory adjustment of the model, in other words the model was adequate for predicting yield of BzH within the range of the variables studied.

To study the interaction of the process variables with BzH yield for catalytic oxidation of BzOH, 2D contour plots obtained from the predicted model and 3D response surface were displayed at Figures S4 and S5. As revealed by the elliptical shape of the contour plot, it is evident that there exist strong correlations between x_1x_3 for the BzH yield (Figure S4B). Correlations between x_1x_2 Figure S4A) or x_1x_4 (Figure S4C), which exhibited circular or scattered contour plots, are less significant. Moreover, based on the results of 3D response surface plots (Figure S5), it is indicated that interaction between x_2x_4 has stronger influence on product yield than that of x_2x_3, or x_3x_4. These observations were in an excellent agreement with ANOVA data (Table 4) and experimental results (Figures S4D–F).

Based on RSM results, a mathematical model predicted an optimal BzH yield of 96.01% for the oxidation of BzOH with H_2O_2 over the $[DMBPSH]H_2PW_{12}O_{40}$ catalyst under the following process conditions: $x_1 = 1{:}1.70$, $x_2 = 5.44$ wt%, $x_3 = 3.93$ h, and $x_4 = 24.10$ ml at a reaction temperature of 393 K. To confirm validity of the model and optimal process conditions, three additional experiments were conducted in parallel at 393 K with $x_1 = 1{:}1.7$, $x_2 = 5.4$ wt%, $x_3 = 3.9$ h, $x_4 = 24$ ml. Accordingly, BzH yields of 96.2%, 95.6%, and 95.7% were obtained, leading to an average experimental yield of 95.8%. The results are in

Table 4: Estimated regression coefficients and corresponding *F*- and p-values for BzH yield.

Source	Sum of squares	DF[a]	Mean square	*F*-value	Prob > *F*	Significance[b]
Model	604.64	14	43.19	49.58	<0.0001	[d]
x_1	165.39	1	165.39	189.87	<0.0001	[d]
x_2	7.65	1	7.65	8.78	0.0103	[c]
x_3	16.83	1	16.83	19.32	0.0006	[d]
x_4	16.38	1	16.38	18.80	0.0007	[d]
x_1^2	322.09	1	322.09	369.76	<0.0001	[d]
x_2^2	26.41	1	26.41	30.32	<0.0001	[d]
x_3^2	61.30	1	61.30	70.37	<0.0001	[d]
x_4^2	51.42	1	51.42	59.03	< 0.0001	[d]
x_1x_2	0.33	1	0.33	0.38	0.5477	
x_1x_3	16.61	1	16.61	19.06	0.0006	[d]
x_1x_4	1.68	1	1.68	1.93	0.1870	
x_2x_3	5.09	1	5.09	5.84	0.0299	[c]
x_2x_4	15.60	1	15.60	17.91	0.0008	[d]
x_3x_4	6.18	1	6.18	7.09	0.0186	[c]
Residual	12.19	14	0.87			
Lack of fit	11.27	10	1.13	4.90	0.0697	
Pure error		0.92	4	0.23		
Cor total		616.84	28			

[a]DF denotes degrees of freedom.
[b,c]Significant; [d]highly significant.

good agreement with the predicted values, hence, once again justifying validity of the proposed model.

3.5 Recycling of the catalyst

In order to reduce the cost of an experiment, it is meaningful to evaluate reusability of [DMBPSH]$H_2PW_{12}O_{40}$ catalyst under the above optimal operation conditions. After each cycle reaction, aqueous phase was subjected to rotary evaporation, and then was dried for 12 h at 348 K under vacuum to create regenerated DMBPS-IL TPA. Results of the catalytic recycling experiment were shown in Figure 3. It revealed that [DMBPSH]$H_2PW_{12}O_{40}$ catalyst was indeed durable after six consecutive experimental cycles without significant losses in conversion and selectivity. The BzH yield and selectivity decreased marginally from 95.8% to 97.0% in the first cycle to 90.7% and 94.8% in the last cycle, respectively. A gradual decrease in catalytic activity observed after repeated cycles was ascribed to leaching TPA. Additional elemental analysis by inductively coupled plasma revealed that concentration of P in the spent catalyst decreased from 0.98 wt% (fresh catalyst) to 0.81 wt% after the sixth run. The above results indicated that [DMBPSH]$H_2PW_{12}O_{40}$ catalyst was not only durable but also recyclable for alcohol oxidation reactions.

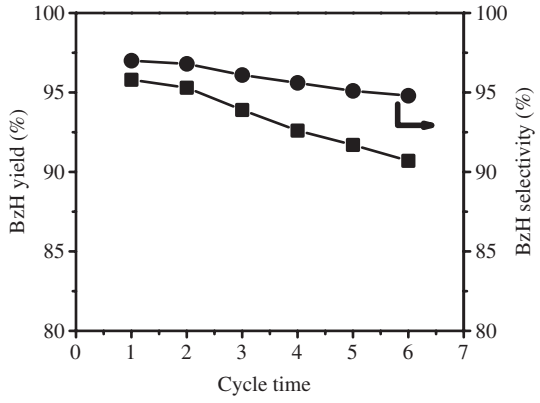

Figure 3: Stability of the [DMBPSH]$H_2PW_{12}O_{40}$ catalyst on BzH yield (■) and BzH selectivity (●) during oxidation of BzOH with H_2O_2.

3.6 Kinetic model development

To demonstrate high accuracy of the kinetic model for the selectivity oxidation of BzOH with [DMBPSH]$H_2PW_{12}O_{40}$ catalyst, a kinetic experiment was conducted under reaction conditions optimized by RSM at different reaction temperatures with different time. Accordingly, reaction rates during the oxidation reaction under varied reactant (BzOH and H_2O_2) concentration were recorded. Based on the simplified rate equation [Eq. (3)], reaction rate (r) can be directly correlated with the rate constant (k) and the concentrations of BzOH (C_A) and H_2O_2 (C_B) with corresponding reaction orders of α and β, respectively, which was defined by Eq. (4). Figures 4A and 5A showed variations of BzOH and H_2O_2 concentrations with time at various initial C_A and C_B values. The concentrations of both reactants decreased linearly with increasing reaction time. Figures 4B and 5B showed a log-log plot of reaction rate and concentration, from which corresponding reaction orders (α and β) may be determined, and the values were 1 and 1.2 for BzOH and H_2O_2, respectively.

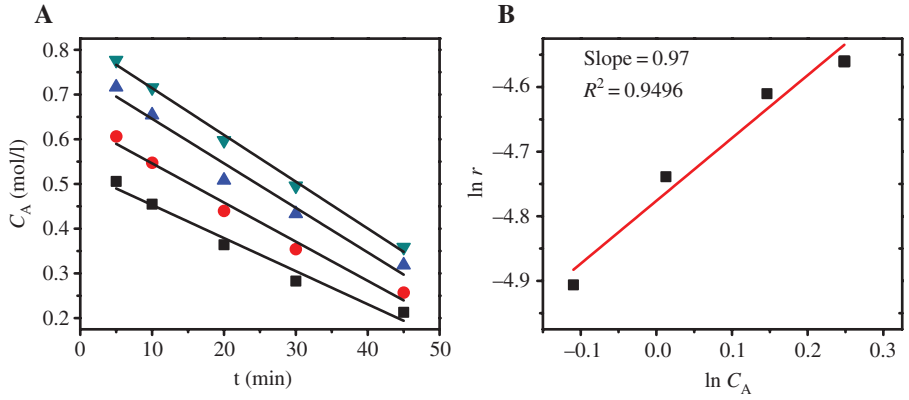

Figure 4: (A) Variations of BzOH concentration (C_A) versus reaction time; symbols for initial C_A values: 1.28 (▼), 1.16 (▲), 1.01 (●), and 0.89 (■) mol/l, and (B) log-log plot of initial oxidation rate versus initial C_A. Reaction conditions: temperature 393 K; initial H_2O_2 concentration 2.18 mol/l; BzH concentration 0 mol/l; and amount of catalyst 7.47 g/l.

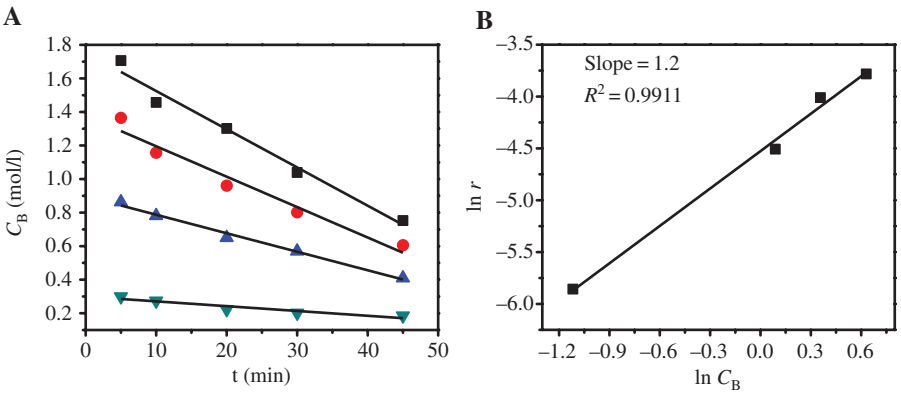

Figure 5: (A) Variations of H_2O_2 concentration (C_B) versus reaction time; symbols for initial C_B values: 1.88 (▼), 1.43 (▲), 1.09 (●), and 0.33 (■) mol/l, and (B) log-log plot of initial oxidation rate versus initial C_A. Reaction conditions: temperature 393 K; initial BzOH concentration 1.28 mol/l; BzH concentration 0 mol/l; amount of catalyst 7.47 g/l.

Figure 6A showed variations of the concentration of BzOH versus reaction time at five different temperatures. As shown in Figure 6A, conversion rate increased with increasing temperature, which indicated that this reaction was controlled by kinetics mode. Moreover, activation energy E_a (kJ/mol) and pre-exponential factor k_0 were attained via linear regression by employing plots of ln k versus $1/T$ based on the temperature dependence of the rate equation, as specified by Eqs (4) and (5). The result was shown in Figure 6B and the activation energy E_a was 36.18 kJ/mol for this oxidation catalyzed by [DMBPSH] $H_2PW_{12}O_{40}$ catalyst. According to the calculated value of E_a and k_0, the Arrhenius equation could be expressed as follows:

$$\ln k = -\frac{4351.4}{T} + 6.50$$

Thus, the kinetic equation for selectivity oxidation of BzOH to BzH under the optimum conditions may be expressed as:

$$r = -\frac{dC_A}{dt} = e^{6.50\left(\frac{-36.18}{RT}\right)} C_A C_B^{1.2}$$

It was worth pointing out that E_a value obtained from the present catalytic system was slightly lower than that of oxidation of vanillyl alcohol to vanillin over N-GO/Mn_3O_4 catalyst (39.67 kJ/mol) [35], but much lower than that observed for the oxidation of furfuryl alcohol over heterogeneous nano zirconium chromate catalyst in tetrahydrofuran (76.68 kJ/mol) [36]. The results indicated that [DMBPSH]$H_2PW_{12}O_{40}$ catalyst was indeed a highly effective catalyst for the oxidation of alcohols to aldehydes and ketones.

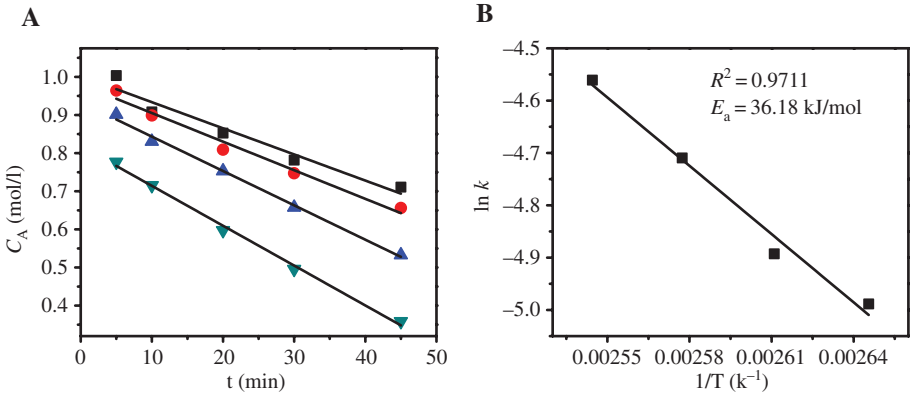

Figure 6: (A) Variations of BzOH concentration versus reaction time under different reaction temperatures: 378 K (■), 383 K (●), 388 K (▲), and 393 K (▼), and (B) the corresponding Arrhenius plot; reaction conditions: initial BzOH concentration 1.28 mol/l; H_2O_2 concentration 2.18 mol/l; and amount of catalyst 7.47 g/l.

4 Conclusions

A series of propyl sulfonic acid-functionalized ionic liquids modified TPA composite catalysts were successfully synthesized and exploited for the oxidation of BzOH in water with H_2O_2. The superior catalytic activity was attributed to high acidity and excellent surface activity of the catalysts. Among various catalysts examined, $[DMBPSH]H_2PW_{12}O_{40}$ catalyst exhibited the best catalytic properties and was employed for process optimization to obtain optimal oxidation conditions at $BzOH/H_2O_2$ molar ratio 1:1.7, catalyst amount 5.4 wt%, reaction time 3.9 h, and 24 ml water, leading to a desirable BzH yield of 95.8%. These optimized experimental values were in good agreement with those predicted by the RSM based on the BBD model. A reaction order of 2.2 and an activation energy of 36.18 kJ/mol were deduced from the kinetic model developed. Additional recyclability study also indicated that DMBPS-IL TPA catalyst was truly efficient and reusable for oxidation of alcohols.

References

[1] Mori K, Yamaguchi K, Hara T, Mizugaki T, Ebitani K, Kaneda K. *J. Am. Chem. Soc.* 2002, 124, 11572–11573.
[2] Azizi N, Khajeh M, Alipour M. *Ind. Eng. Chem.* Res. 2014, 53, 15561–15565.
[3] Arena F, Guminab B, Lombardo AF, Espro C, Patti A, Spadaro L, Spiccia L. *Appl. Catal. B Environ.* 2015, 162, 260–267.
[4] Choudary BM, Kantam ML, Rahman A, Reddy CV, Rao KK. Angew. *Chem. Int. Ed.* 2001, 40, 763–766.
[5] Steinhoff BA, Fix SR, Stahl SS. *J. Am. Chem. Soc.* 2002, 124, 766–767.
[6] Brink GJ, Arends IWCE, Sheldon RA. *Science* 2000, 287, 1636–1639.
[7] Tundo P, Romanelli GP, Vázquez PG, Aricò F. *Catal. Commun.* 2010, 11, 1181–1184.
[8] Zhang S, Zhao G, Gao S, Xi Z, Xu J. *J. Mol. Catal. A Chem.* 2008, 289, 22–27.
[9] Pathan S, Patel A. *Appl. Catal. A: Gen.* 2013, 459, 59–64.
[10] Zhu SH, Gao XQ, Dong F, Zhu YL, Zheng HY, Li YW. *J. Catal.* 2013, 306, 155–163.
[11] Zhou L, Al Zaini E, Adesina AA. *Fuel* 2013, 103, 617–625.
[12] Misono M. *Catal. Today* 2009, 144, 285–291.
[13] Han XX, He YF, Hung CT, Liu LL, Huang SJ, Liu SB. *Chem. Eng. Sci.* 2013, 104, 64–72.
[14] Huang MY, Han X, Hung CT, Lin JC, Wu PH, Wu JC, Liu SB. *J. Catal.* 2014, 320, 42–51.
[15] Han XX, Zhang XF, Zhu GQ, Liang JJ, Cao XH, Kan RJ, Hung CT, Liu LL, Liu SB. *ChemCatChem* DOI:10.1002/cctc.201600788.
[16] Leng Y, Jiang P, Wang J. *Catal. Commun.* 2012, 25, 41–44.
[17] Leng Y, Zhao P, Zhang M, Wang J. *J. Mol. Catal. A Chem.* 2012, 358, 67–72.
[18] Sloboda-Rozner D, Alsters PL, Neumann R. *J. Am. Chem. Soc.* 2003, 125, 5280–5281.
[19] Carraro M, Bassil BS, Soraru A, Berardi S, Suchopar A, Kortz U, Bonchio M. *Chem. Commun.* 2013, 49, 7914–7916.
[20] Hua L, Qiao Y, Yu Y, Zhu W, Cao T, Shi Y, Li H, Feng B, Hou Z. *New J. Chem.* 2011, 35, 1836–1841.
[21] Han XX, Zhou LX. *Chem. Eng. J.* 2011, 172, 459–466.
[22] Han XX, Chen KK, Yan W, Hung CT, Liu LL, Wu PH, Lin KC, Liu SB. *Fuel* 2016, 165, 115–122.
[23] Montgomery DC. *Design and Analysis of Experiments*, 5th ed., John Wiley and Sons: New York, 2001.
[24] Han XX, Du H, Hung CT, Liu LL, Wu PH, Ren DH, Huang SJ, Liu SB. *Green Chem.* 2015, 17, 499–508.
[25] Rao PM, Wolfson A, Kababya S, Vega S, Landau MV. *J. Catal.* 2005, 232, 210–225.
[26] Santos FM, Brandão P, Félix V, Cavaleiro AMV, de Matos Gomes E, Belsley MS. *J. Mol. Struct.* 2010, 963, 267–273.
[27] Huang SJ, Yang CY, Zheng A, Feng N, Yu N, Wu PH, Chang YC, Lin YC, Deng F, Liu SB. *Chem. Asian J.* 2011, 6, 137–148.
[28] Zheng A, Li S, Liu SB, Deng F. *Acc. Chem. Res.* 2016, 49, 655–663.
[29] Zheng A, Huang SJ, Chen WH, Wu PH, Zhang H, Lee HK, de Ménorval LC, Deng F, Liu SB. *J. Phys. Chem. A* 2008, 112, 7349–7356.
[30] Gui JZ, Liu D, Sun ZL, Liu DS, Min DY, Song BS, Peng XL. *J. Mol. Catal. A Chem.* 2010, 331, 64–70.
[31] Li XZ, Cao R, Lin Q. *Catal. Commun.* 2015, 69, 5–10.
[32] Yang X, Wang X, Liang C, Su W, Wang C, Feng Z, Li C, Qiu J. *Catal. Commun.* 2008, 9, 2278–2281.
[33] Liu LM, McAllister B, He HQ, Hu P. *J. Am. Chem. Soc.* 2006, 128, 4017–4022.
[34] Bongiorno A, Landman U. *Phys. Rev. Lett.* 2005, 95, 106102–106104.
[35] Yuan ZL, Chen SH, Liu B. *J. Mater. Sci.* 2017, 52, 164–172.
[36] Setareh S, Nooredin G. *Monatsh. Chem.* 2016, 147, 1531–1538.

Supplemental Material: The online version of this article (DOI: 10.1515/gps-2016-0237) offers supplementary material.

Bionotes

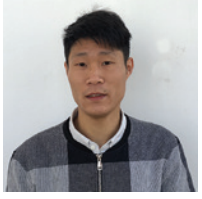

Ouyang Kai

Ouyang Kai is a graduate student in the Department of Applied Chemistry, Zhejiang Gongshang University.

Han Xiaoxiang

Han Xiaoxiang received a PhD degree from the Department of Chemistry, Zhejiang University in 2004. He is an associate professor and works as a supervisor of Master's degrees in the Department of Applied Chemistry, Zhejiang Gongshang University.

Xiong Chunhua

Xiong Chunhua graduated from HuNan University. He is a professor in the Department of Applied Chemistry, Zhejiang Gongshang University.

Tang Xiujuan

Tang Xiujuan completed the doctoral program at Zhejiang University in 2008 and subsequently joined the faculty as an assistant researcher. Since 2011, she has been a lecturer at Zhejiang Gongshang University.

Chen Qing

Chen Qing received a PhD degree from the Department of Chemistry, Zhejiang University in 2006. She is an associate professor in the Department of Applied Chemistry, Zhejiang Gongshang University.